Journal of Cellular Biochemistry 83:643–659 (2001)

Distribution of Somatic H1 Subtypes is Non-Random on Active vs. Inactive Chromatin II: Distribution in Human Adult Fibroblasts

Missag H. Parseghian,[1] Robert L. Newcomb,[2] and Barbara A. Hamkalo[1]*

[1]Department of Molecular Biology and Biochemistry, University of California, Irvine, Irvine, California 92697
[2]The UCI Center for Statistical Consulting, University of California, Irvine, Irvine, California 92697

Abstract For nearly twenty years researchers have observed changes in the histone H1 subtype content of tissues as an organism develops into an adult. To better understand the consequences of such changes, immunofractionation of chromatin using previously characterized antibodies specific for human H1 subtypes was employed in the analysis of a fibroblast cell strain derived from a 37-year-old individual. DNAs isolated from immunoprecipitates were probed for the existence of a variety of DNA sequences. The results presented lend further support to a previously-proposed model (Parseghian et al. [2000] Chromosome Res 8:405-424) in which transcription of a sequence is accompanied by the selective depletion of subtypes. The data also suggest that there is more total H1 on actively transcribed sequences in these cells as compared to fetal fibroblasts and that there is less difference in the subtype compositions of active genes vs. inactive sequences in this strain. Specifically, the consequences of these changes appear to correlate with the attenuation of the heat shock response in aging fibroblasts. In a broader context, these results could explain why there are reductions in transcription in cells from mature tissue that approach senescence. J. Cell. Biochem. 83: 643–659, 2001.

Key words: histone h1; chromatin organization; heat shock; development; aging

There is evidence in the literature that there are changes in nuclear structure and function that correlate with cellular development and subsequent aging. Such changes are evident at the earliest stages of embryogenesis in higher eukaryotes from amphibians [Dimitrov et al., 1993] to mammals [Wiekowski et al., 1997]. For example, the transition from maternal to zygotic gene expression is accompanied by an increased repression of replication origins and transcriptional promoters that correlate with shifts in histone H1 subtype content [Dimitrov et al., 1993] and core histone deacetylation [Wiekowski et al., 1997]. In amphibian embryos, the transition from an oocyte-specific linker histone to a family of somatic H1 subtypes (designated $H1^S$) [Parseghian et al., 1994a] causes a loss of mesodermal tissue induction [Steinbach et al., 1997]. Changes have also been observed in the somatic H1 subtype content of developing cells and organs well into adulthood [e.g. Lennox and Cohen, 1983; Pina et al., 1987; and as reviewed in Parseghian and Hamkalo, 2001], however, these changes have not been correlated with changes in nuclear function.

Cellular aging has been correlated with decreases in the transcriptional induction of certain genes [e.g. Liu et al., 1989a; Luce and Cristofalo, 1992] as well as decreases in the overall expression of others [e.g. Wang et al., 1997]. However, the effects of aging are not limited to actively transcribed genes. Chaurasia et al. [1996] report increased chromatin condensation of satellite DNA in liver cells of older rats when compared to younger animals. In addition, aging cells display changes in nuclear morphology and a loss of mitotic activity

Abbreviations used: ANOVA, analysis of variance; $H1^S$, somatic H1 subtype; SIP, signal intensity percentage.

Grant sponsor: NSF to BAH; Grant number: MCB9302219.

Missag H. Parseghian's present address is Research and Development, Peregrine Pharmaceuticals, 14272 Franklin Ave., Tustin, CA 92780.

*Correspondence to: Barbara A. Hamkalo, Department of Molecular Biology and Biochemistry, University of California, Irvine, Irvine, CA 92697. E-mail: bahamkal@uci.edu

Received 27 February 2001; Accepted 10 May 2001

DOI 10.1002/jcb.1224

generally referred to as replicative senescence [Hayflick and Moorhead, 1961]. Senescence is a dominant phenotype mediated by unknown cellular factor(s) that inhibit(s) replication in younger cells upon fusion with senescent cells [Norwood et al., 1974]. Despite these observations, the mechanism(s) underlying these changes still remain unclear. The effects of aging on replication and transcription may involve changes in chromatin organization. Since histone H1 plays a critical role in the maintenance of higher order chromatin structure [reviewed in van Holde, 1988], the general repression of transcription [Shimamura et al., 1989; Croston et al., 1991; Laybourn and Kadonaga, 1991], and the inhibition of replication [Lu et al., 1997, 1998, 1999], understanding possible changes in the H1 subtype composition of nuclei as cells develop and age may lead to insights into both processes.

Based on chromatin immunoprecipitations using subtype-specific antibodies, we proposed a model for the preferential depletion of subtypes $H1^S$-2 and $H1^S$-4 in actively transcribed chromatin [Parseghian et al., 2000]. In contrast, $H1^S$-3 is present on active *and* inactive chromatin. The depletion of specific subtypes on actively transcribed chromatin may contribute to a more open chromatin conformation that allows access to transcription factors, as evidenced by Hannon et al. [1984], who observed greater repression of RNA polymerase initiation after reconstitution of H1-depleted chromatin with total H1 than with isolated subtypes at identical concentrations.

In light of our recent observations [Parseghian et al., 2000], the current paper analyzes somatic H1 distributions in a karyotypically normal diploid cell strain (GM1653) derived from the skin fibroblasts of a 37-year-old male [Case and Wallace, 1981]. Earlier observations of distinct differences in subtype distributions on active and inactive chromatin are confirmed. As noted above, active genes are dramatically depleted of certain subtypes whereas inactive sequences possess most or all subtypes. Interestingly, the cells derived from adult tissue have a reduction in these differences so that active chromatin possesses a more heterogenous distribution of subtypes, as well as an overall increased amount of total H1. The possibility that such changes lead to replicative senescence is discussed. Also, the effect of such changes on the induction of heat shock genes are analyzed. Results presented suggest H1 may play a role in the mechanism of an attenuated transcriptional response with age [as reviewed in Liu et al., 1996].

MATERIALS AND METHODS

Cell Growth and Chromatin Immunoprecipitation

The karyotypically normal human diploid fibroblast strain (GM1653), purchased from the NIGMS Human Genetic Mutant Cell Repository, was derived from the skin fibroblasts of a 37-year-old male [Case and Wallace, 1981]. Cell growth, DNA labeling, formaldehyde crosslinking, chromatin isolation, immunoprecipitation, and analysis procedures were previously described [Parseghian et al., 2000]. Briefly, cells were grown at 37°C in Dulbecco's Modified Eagle Medium (DMEM) (GibcoBRL, Gaithersburg, MD), and the DNA labeled at ~75% confluency by the addition of (methyl-^{3}H) thymidine (79 Ci/mmol, Amersham, Piscataway, NJ) at a concentration of 1 μCi/ml of media. After 36–72 h of incubation, the tritium-labelled chromatin was crosslinked and sonicated then immunoprecipitated with polyclonal antibodies generated against one of four somatic H1 subtypes or with an antibody against all of the subtypes (designated anti-total H1). Production and characterization of the rabbit polyclonal antibodies against the H1s has been described previously [Parseghian et al., 1993, 1994b].

Immunoprecipitation with rabbit preimmune antibodies was used as a control in order to determine the amount of background signal during PCR and slot blotting. All pre-immune antibodies used for experimentation did not crossreact with any H1 subtypes as verified by Western analysis (data not shown). Hence, any background signals could be due to a low-level crossreactivity of protein G to core histones similar to that documented for protein A [Hebbes et al., 1988]. Once precipitated, bound RNA and proteins were hydrolyzed and then the crosslinks reversed by incubation at 65°C for at least 6 h. As a second control, a batch of chromatin prior to immunoprecipitation was similarly treated in order to have a sample of input DNA. Equal quantities of the DNA obtained were subsequently analyzed for the presence of various transcriptionally active and inactive sequences using PCR or slot blotting, such

analyses for any sequence being repeated, with different chromatin preparations, from 3–5 times. A third control monitored the consistency of the PCR by the inclusion in each reaction of 0.5 pg Bluescript plasmid (Stratagene, La Jolla, CA). A 126 bp sequence was amplified using 0.5 μM of modified Bluescript primers [Parseghian et al., 2000]. Finally, a fourth control involved the preparation of a polymerase chain reaction mixture containing no template DNA in order to check for DNA contamination from external sources.

Several observations argue against the possibility of limiting reagent quantities in the PCR reactions (i.e., the so-called "Plateau Effect") [Innis and Gelfand, 1990]. Reactions in the plateau phase should result in signal patterns that are indistinguishable between active and inactive chromatin; however, as detailed below, ANOVA analyses statistically verify the significant difference in signals from each class of DNA. The possibility of a plateau effect also is inconsistent with the heat shock data in which reproducible shifts in signal patterns are demonstrated for the functional HSP90α gene. As a further check on the validity of signal patterns, the PCR results for active and inactive chromatin were independently verified in this and the previous study by slot blot analysis where there is no plateau effect.

DNA Probes and Primers

Plasmid pXBR-1, a human α-satellite DNA probe, was previously characterized [Yang et al., 1982]. The telomeric repeat sequence was a gift from Dr. Robert Moyzis [Moyzis et al., 1988]. Other oligonucleotide primers were gifts from Drs. Leslie Thompson (FGFR-3), Marian Waterman (LEF-1) and Dean Stathakis (PSD95). Primer sequences, concentrations and annealing temperatures are listed in Parseghian et al. [2000].

Data Analysis

Gels (PCR) and films (slot blots) were digitized using the Image Store 5000 Gel Documentation System (UVP, San Gabriel, CA) and analyzed using Gelbase software (also UVP). Digitizing allows for a pixel-by-pixel analysis of the signal intensity from each band, hence, intensities of the bands resulting from each of the four subtype-specific immunoprecipitations and the preimmune control were determined. After subtraction of the preimmune signal intensity, each of the resulting four subtype values were totalled, and the signal intensity percentage (SIP) for each subtype determined. The assays employing PCR included the signal generated from a 126 bp Bluescript band as an internal control. In each experiment, the control band with the least total signal intensity was assigned a value of 100% and the remaining control bands assigned percentage values relative to it. Comparisons of the relative intensity of the control bands across lanes in a single experiment were used to evaluate the consistency of amplification. When differences of two- or three-fold in signal were seen for the internal control in a single experiment, the experiment was repeated.

The significance of the signal intensity data was statistically verified by analysis of variance (ANOVA) using the SAS software package (SAS Institute, Cary, NC). All SIPs were categorized according to the following parameters: H1 subtype and the transcriptional state of the DNA being analyzed. Several omnibus and focus tests, using combinations of the two parameters, compared mean SIPs and determined the statistical significance of their deviation from an expected null hypothesis value of 25%.

RESULTS AND DISCUSSION

General Remarks

This paper focuses on GM1653, a skin fibroblast strain with a normal diploid karyotype. Its origin from a 37-year-old makes this cell strain a suitable candidate for analyzing changes in nuclear structure and function during development and aging. Henceforth, it will be referred to as the adult fibroblast line. In addition, these cells allow us to focus exclusively on the somatic subtypes because they lack two differentiation-specific isoforms: $H1^{o}$, a variant generally present in quiescent cells, and H1a, a subtype enriched only in testis and thymus [Burfeind et al., 1992].

An earlier study of somatic H1 subtype distributions in fetal fibroblast cells describes the crosslinking and immunoprecipitation strategies [Parseghian et al., 2000]. The SIP (signal intensity percentage) for each subtype was determined by analysis of computer digitized gels and films generated during PCR and slot blot studies, respectively. The average SIPs reported here are derived from repeated analyses

of each DNA sequence studied, and are accompanied by a sample gel or blot. The gels and blots are provided as examples of the qualitative trends observed, while the average SIPs present the results in a semi-quantitative manner that describes the trends. Studying the same genes and sequences as in the fetal fibroblast study permitted comparisons between the two cell strains and provided a broad sampling of expression patterns and a diversity of chromosomal sites in the adult fibroblasts. The transcriptional state of each sequence was confirmed by reverse-transcriptase (RT) PCR or northern analysis (data not shown).

The current study and its earlier companion are driven by the following hypothesis: If H1 subtypes do possess distinct functions, then a non-random distribution would be predicted on different classes of DNA, such as active and inactive genes. On the other hand, the null hypothesis states that no significant differences in H1 subtype content should exist between active vs. inactive regions of chromatin. Furthermore, if the distribution of subtypes is truly random in the nucleus, then approximately equal SIPs, of about 25%, should be observed from each of the four subtypes, irrespective of the DNA sequence.

Although results from different DNA sequences were generally reproducible, there is variability inherent in the immunoprecipitation assay so that, while qualitative trends are apparent, our semi-quantitative data was supplemented with statistical analysis. To address this, all of the data was subjected to a comprehensive ANOVA (see below).

Distribution of Subtypes on Transcriptionally Active Chromatin: PSD95 & c-myc

The investigation of subtype associations on active chromatin involved constitutively-expressed (PSD95) and inducible (c-myc) genes. PCR analysis of the actively transcribed genes demonstrate the greatest SIPs from subtypes $H1^S$-3 and $H1^S$-1, while average SIPs due to $H1^S$-2 are well below 20% (Fig. 1A). Although the pattern of subtype distributions is reminiscent of our previous observations, in which active chromatin exhibited a selective depletion of subtypes [Parseghian et al., 2000], when these results are compared to those from fetal fibroblasts, the $H1^S$-3 SIP is lower whereas the $H1^S$-1 SIP is higher. Thus, it appears that there is a decrease in the predominance of one subtype in active chromatin with age, resulting in a gradual reduction in differences in the subtype compositions of active and inactive sequences. This modest decrease in average SIPs for $H1^S$-3 is not necessarily a reflection of its greatly reduced amount in quiescent, adult tissues as reported by others [Lennox and Cohen, 1983; Wang et al., 1997], since these cells are still proliferating. In fact, $H1^S$-3 is quite prevalent in this cell strain, nearly equaling the quantity of $H1^S$-1 at about 38%.

Distribution of Subtypes on Transcriptionally Inactive Chromatin: LEF-1, IgKC & FGFR3

Lymphoid enhancer-binding factor-1 (LEF-1) and immunoglobulin kappa constant region (IgKC), were used as representatives of inactive sequences. Figure 1B shows that both genes have average SIPs for $H1^S$-3 that are far less than those of active chromatin, with a greater preponderance of signal from $H1^S$-2 (as evidenced by average SIPs greater than 40%) and to some extent from $H1^S$-4. These results are consistent with those obtained with fetal fibroblasts. In fact, no $H1^S$-3 appears to associate with IgKC in GM1653 cells, further supporting earlier observations that suggest the preferential association of the other subtypes with inactive chromatin [Parseghian et al., 2000].

Although fibroblast growth factor receptor-3 (FGFR-3) is expressed in many fibroblast lines [Thompson et al., 1991], it is transcriptionally silent in the cell strains used in this and our previous study (Fig. 5A). Therefore, the increased association of $H1^S$-3 was unexpected (Fig. 1B). However, we observed induction of FGFR-3 upon heat shock in both the fetal and adult cell lines, indicating that it is poised for transcription rather than irreversibly repressed (Fig. 5A). The average SIP for $H1^S$-3 is nearly 40%, while $H1^S$-1 and $H1^S$-2 are nearly 25%, in both fibroblast strains despite the difference in age of the sources. Therefore, despite the increased heterogeneity of subtypes present on this gene, the prevalence of $H1^S$-3 on a gene may be indicative of its potential to be transcribed with additional changes in subtype content upon transcriptional induction (see below).

Several indirect lines of evidence suggest that $H1^S$-3 prevalence on a sequence may indicate a more open chromatin conformation. For example, in mouse fibroblasts, phosphorylated $H1^S$-3 has been colocalized to RNA processing sites

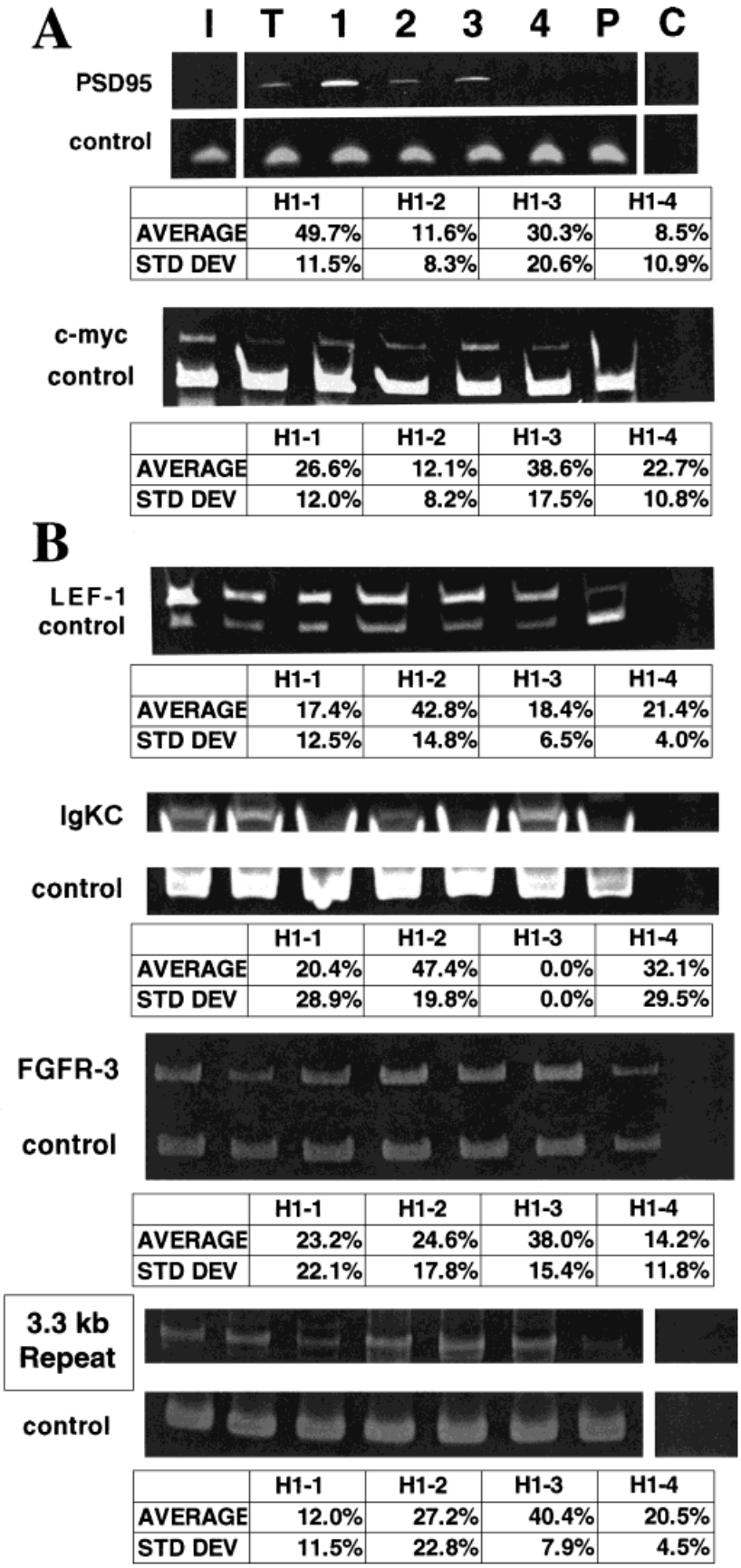

	H1-1	H1-2	H1-3	H1-4
AVERAGE	49.7%	11.6%	30.3%	8.5%
STD DEV	11.5%	8.3%	20.6%	10.9%

	H1-1	H1-2	H1-3	H1-4
AVERAGE	26.6%	12.1%	38.6%	22.7%
STD DEV	12.0%	8.2%	17.5%	10.8%

	H1-1	H1-2	H1-3	H1-4
AVERAGE	17.4%	42.8%	18.4%	21.4%
STD DEV	12.5%	14.8%	6.5%	4.0%

	H1-1	H1-2	H1-3	H1-4
AVERAGE	20.4%	47.4%	0.0%	32.1%
STD DEV	28.9%	19.8%	0.0%	29.5%

	H1-1	H1-2	H1-3	H1-4
AVERAGE	23.2%	24.6%	38.0%	14.2%
STD DEV	22.1%	17.8%	15.4%	11.8%

	H1-1	H1-2	H1-3	H1-4
AVERAGE	12.0%	27.2%	40.4%	20.5%
STD DEV	11.5%	22.8%	7.9%	4.5%

Fig. 1. PCR analysis. For PCR analyses, immunoprecipitated samples of equal amounts of DNA were amplified according to the protocol described in Parseghian et al. [2000]. Electrophoresis of the resulting PCR products on a 6% acrylamide gel was followed by ethidium bromide staining. Half a picogram of Bluescript plasmid was included as a internal control in each reaction, except for the negative control lane. A pixel-by-pixel analysis of the signal intensity from each band was conducted by digitizing the gels. Each of the resulting four subtype values (minus the preimmune's signal value) were totaled and the signal intensity percentage (SIP) for each determined. Each analysis was repeated, with different chromatin preparations, 3–5 times. Average SIPs and sample gels are shown for transcriptionally (**A**) active and (**B**) inactive sequences. I, Input DNA; T, anti-Total H1; 1, anti-H1^s-1; 2, anti-H1^s-2; 3, anti-H1^s-3; 4, anti-H1^s-4; P, Preimmune antibodies; and C, negative control for PCR.

[Chadee et al., 1995], and $H1^S$-3 exhibits the greatest level of cyclin-dependent phosphorylation [Talasz et al., 1996]. In addition, with the exception of $H1^S$-1, $H1^S$-3 is preferentially poly(ADP-ribosyl)ated as compared to the other somatic variants [Riquelme et al., 1979; D'Erme et al., 1996].

In general, a comparison of the subtype content for selected active and inactive sequences reveals a more heterogenous presence of somatic subtypes on inactive chromatin. However, unlike fetal fibroblasts, the subtype content of transcriptionally inactive DNA does not as closely approach the equal distribution of signals for each subtype (~25%). While both $H1^S$-2 and to a lesser extent, $H1^S$-4 appear to be more prevalent with inactive regions of chromatin, the increased presence of the former consistently correlates with transcriptional inactivity: the SIPs for $H1^S$-2 from LEF-1 and IgKC are >40%, a larger percentage than that seen for the same genes in fetal fibroblasts (>30%). Comparison of these to the average SIPs for actively transcribed c-myc; shows that the presence of $H1^S$-2 is considerably reduced (12%), while $H1^S$-4 still averages 22.7%. A decrease in expression of c-myc as these adult cells approach senescence may account for the greater than expected value for $H1^S$-4.

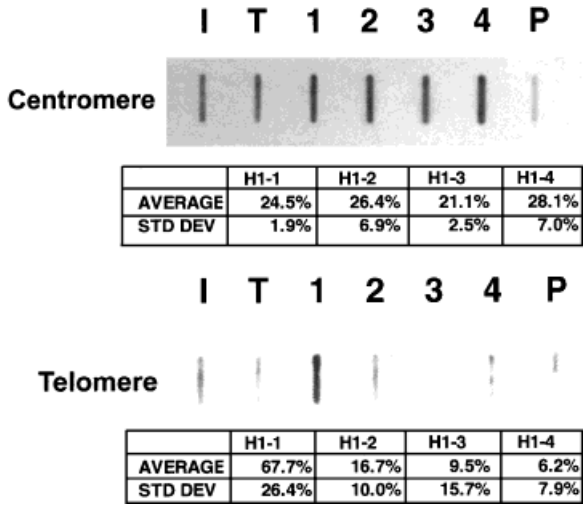

	H1-1	H1-2	H1-3	H1-4
AVERAGE	24.5%	26.4%	21.1%	28.1%
STD DEV	1.9%	6.9%	2.5%	7.0%

	H1-1	H1-2	H1-3	H1-4
AVERAGE	67.7%	16.7%	9.5%	6.2%
STD DEV	26.4%	10.0%	15.7%	7.9%

Fig. 2. Slot Blot analysis. Equal amounts of DNA from the immunoprecipitated samples were denatured, applied to nylon membranes and UV crosslinked according to the protocol described in Parseghian et al. [2000]. A non-radioactive detection system (Genius System from Boehringer) utilizing digoxigenin-labelled probes was used to record the results on film. An α-satellite DNA probe [Yang et al., 1982] and a telomeric repeat sequence [Moyzis et al., 1988] were used for detection of centromeric and telomeric DNA, respectively. A pixel-by-pixel analysis of the signal intensity from each band was conducted by digitizing the blots. Each of the resulting four subtype values (minus the preimmune's signal value) were totaled and the SIP for each determined. Each analysis was repeated, with different chromatin preparations, 3–5 times. Average SIPs and sample blots are shown. I, Input DNA; T, anti-Total H1; 1, anti-$H1^s$-1; 2, anti-$H1^s$-2; 3, anti-$H1^s$-3; 4, anti-$H1^s$-4; P, Preimmune antibodies.

Distribution of Subtypes on Centromeric Satellite Repeats

Due to their high copy number, α-satellite repeats were analyzed by slot blotting. The distribution of SIPs on these sequences are distinctly different when compared to results with active chromatin (Fig. 2). That is, there are approximately equal signal intensities for each subtype, indicating maximum subtype heterogeneity in this region of the genome. A comparison of these data with results from fetal fibroblasts, where the α-satellite SIPs for $H1^S$-3 are over 30% [Parseghian et al., 2000], indicates that the decrease in the predominance of $H1^S$-3 SIPs with aging is not restricted to active chromatin. In light of the model we recently proposed suggesting that $H1^S$-3 prevalence on a sequence may be a good indicator of a more open chromatin conformation, one would predict that the slightly increased subtype heterogeneity present on the adult heterochromatin would contribute to a more condensed conformation than that present on the fetal heterochromatin. This prediction is consistent with recent observations by Chaurasia et al. [1996] who showed overall condensation of bulk chromatin in aging rats, with a specific increase of satellite DNA in the insoluble chromatin fraction.

Distribution of Subtypes on Telomeric and Subtelomeric Repeats

Contrary to the overall trends described for chromatin, where inactive sequences have a diverse subtype content; telomeric heterochromatin in adult cells displays striking differences to both fetal telomeres, and other adult inactive sequences. Whereas the SIP distribution of repeats in fetal fibroblasts had the subtype heterogeneity characteristic of inactive chromatin [Parseghian et al., 2000], nearly 70% of SIPs in adult cells were concentrated in one subtype ($H1^S$-1, Fig. 2). Uneven loading of immunoprecipitated DNA is an unlikely expla-

nation for the distinct SIP pattern seen with the telomeric probe for several reasons. First, each of the slot blots was the result of an independent chromatin preparation. Second, incubation of each blot with the telomeric probe was either preceeded by or followed with the stripping of probe and rehybridization with the centromeric sequence probe, which demonstrated an equal distribution of signal from all four subtypes (Fig. 2). Although telomeric repeats appear to have a lower total H1 content than inactive chromatin in general, there appears to be a further reduction in adult tissue (see Total H1 Content section below). Results from Bedoyan et al. [1996] are consistent with this observation since they showed that only a minority of telomere-sequence mononucleosomes from nonfetal rat liver nuclei contain H1. The same group also provided evidence for a shorter nucleosome repeat length in telomeres compared to bulk chromatin, a result that could be due to H1 depletion [Makarov et al., 1993]. Recently, similar observations have been reported in the plant *Arabidopsis thaliana* where the stoichometry of linker histones to nucleosomes in telomeres are significantly reduced in comparison to bulk chromatin [Ascenzi and Gantt, 1999].

The results for telomeric repeats appear to contradict our model. However, the establishment of a less condensed chromatin conformation could provide an opportunity for telomere-specific factors to access these sequences, much as regions of H1-depleted active chromatin allow access to transcriptional regulatory factors. Telomere-associated factors could include telomere-binding proteins and, possibly, proteins involved in their attachment to the nuclear envelope. Support for such a scenario is derived from the recent characterization of tankyrase, a poly(ADP-ribose) polymerase (PARP), which complexes with the telomeric-repeat binding factor TRF1 [Smith et al., 1998]. PARP activity has been correlated to the modulation of chromatin condensation by H1 [de Murcia et al., 1986; Huletsky et al., 1989], as well as the maintenance of telomeric stability [d'Adda di Fagagna et al., 1999]. In fact, preferential poly(ADP-ribosyl)ation of $H1^S$-1 has been noted in several earlier publications [Riquelme et al., 1979; Parseghian et al., 1994b; D'Erme et al., 1996], rendering the predominance of $H1^S$-1 on telomeric DNA even more intriguing. Such modifications as poly(ADP-ribosyl)ation offer a greater range of chromatin condensation levels, allowing for refinement of the coarse regulation established by the H1s.

The results we see with these telomeric sequences led us to investigate the subtype composition in sub-telomeric repeats. We probed for a specific 3.3 kb tandem repeat that has been localized to subtelomeric regions 4q and 10q [Winokur et al., 1994]. Extensive characterization has revealed that the sequence, packaged as heterochromatin, is immediately adjacent to euchromatin. As a paradox, the euchromatin adjoining most telomeres in the human genome is more transcriptionally and recombinationally active than other heterochromatin-linked sequences [Saccone et al., 1992]. In the case of the 3.3 kb repeat, the SIPs for $H1^S$-3 average 40%, while those for $H1^S$-4 average 20% and $H1^S$-2 exceed 25% (Fig. 1B). Reminiscent of FGFR-3, the heterogeneity of subtypes present and the greater $H1^S$-3 content may be indicative of sequences with the potential to have a more open chromatin conformation.

Distribution of Subtypes on Genes and Pseudogenes

The heat shock protein 90α (HSP90α) gene family was chosen in order to compare subtype distributions on the active and inactive copies of the same gene. The family includes one functional gene and three pseudogenes, each located on a different chromosome [Hickey et al., 1989; Ozawa et al., 1992; Vamvakopoulos et al., 1993]. Primers for PCR amplification were designed to distinguish between gene and pseudogenes [Parseghian et al., 2000].

The distribution of SIPs for the pseudogenes resembled those of centromeric heterochromatin—a quarter of the total signal was obtained from each of the four subtypes (Fig. 3A). However, the distribution differed for the functional gene (Fig. 3B): an overall analysis of SIP averages shows a pattern similar to that of actively transcribed genes with the greatest percentages from subtypes $H1^S$-3 (46.2%) and $H1^S$-1 (28.5%), and mean SIPs for $H1^S$-2 slightly below 20% and $H1^S$-4 well below 10%. Interestingly, PCR analysis of the functional gene using chromatin harvested from cells at successive increased passages showed a shift in subtype patterns. The signal distributions appear to evolve from a predominance of $H1^S$-3 to an increased presence of $H1^S$-2 (Fig. 3B). A more dramatic reflection of the shifting subtype

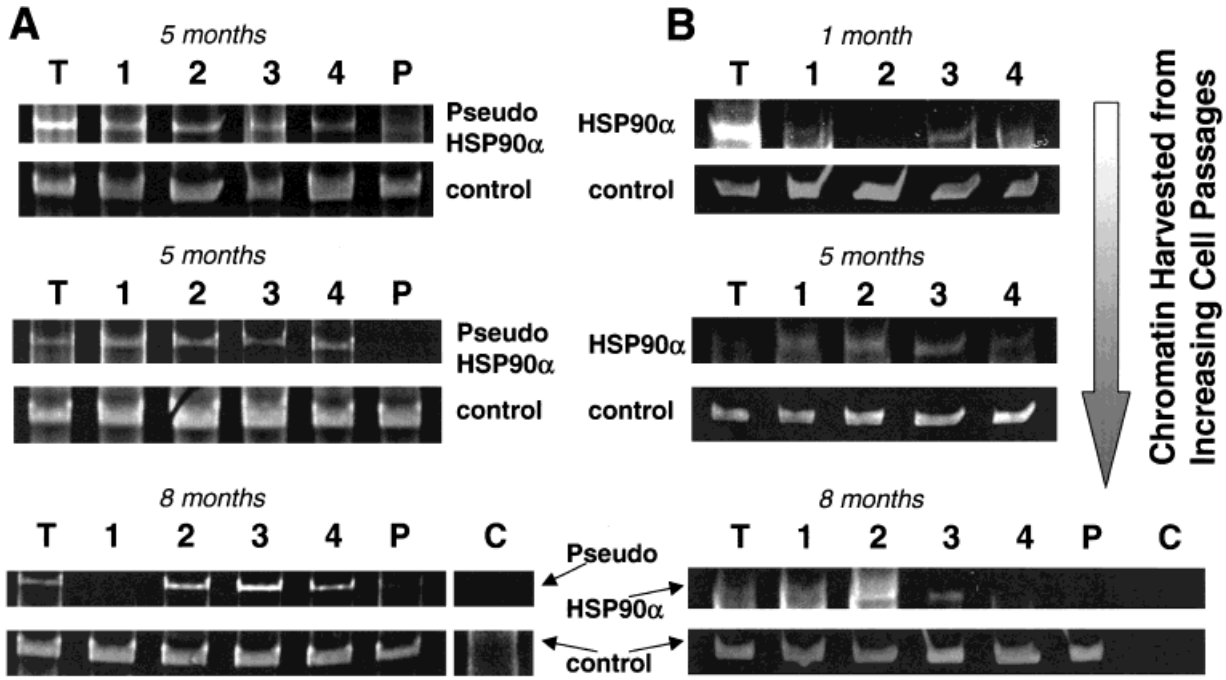

	H1-1	H1-2	H1-3	H1-4
AVERAGE	19.7%	28.1%	26.8%	25.4%
STD DEV	20.2%	7.9%	13.2%	11.0%

	H1-1	H1-2	H1-3	H1-4
AVERAGE	28.5%	19.4%	46.2%	5.9%
STD DEV	5.1%	14.8%	22.9%	4.3%

Fig. 3. Analysis of HSP90α. Immunoprecipitated samples of equal amounts of DNA were amplified according to the protocol detailed in Parseghian et al. [2000]. Electrophoresis of the resulting PCR products on a 6% acrylamide gel was followed by ethidium bromide staining. Half a picogram of Bluescript plasmid was included as an internal control in each reaction, except for the negative control lane. A pixel-by-pixel analysis of the signal intensity from each band was conducted by digitizing the gels. Each of the resulting four subtype values (minus the preimmune's signal value) were totaled and the SIP for each determined. Each analysis was repeated, with different chromatin preparations, 3–5 times. Average SIPs and gels are shown from analyses of HSP90α pseudogenes (**A**) and the functional gene (**B**) using chromatin harvested from increasing passages of the cell line. The number of months from initiation of cell culture to chromatin harvest are indicated above each gel. Legend abbreviations are identical to Figure 1.

content associated with HSP90α as an organism develops is apparent in a comparison of the SIPs from the adult vs. fetal fibroblasts. The functional gene has a predominance of signal from $H1^S$-3 (average SIP = 46.2%), although not quite as high as the mean SIP for $H1^S$-3 seen in the fetal cells (69.1%) [Parseghian et al., 2000]. However, a comparison of mean SIPs for $H1^S$-2 from the fetal (8.4%) and adult (19.4%) cell lines indicates a nearly 2.5-fold increase in this subtype on the functional gene in the adult line approaching senescence.

Distribution of Subtypes on a Heat Shock Gene Upon Induction

HSP90α was further investigated for a better understanding of effects on the subtype composition of a gene upon induction. Although constitutively expressed, transcription of HSP90α increases during cellular stress. Interestingly, the magnitude of induction appears to decrease with age. For example, one study determined a 22-fold increase in mRNA within 3 h of induction in early passage fibroblasts but only a 9-fold increase occurring within 6 h in late passage fibroblasts [Liu et al., 1989b]. In order to investigate this further, GM1653 cells were heat shocked by incubation at 42°C for 1.5 to 2 h followed by the standard analysis.

Heat shock of the adult fibroblast line resulted in a significant shift in subtype content from a predominance of $H1^S$-3 and $H1^S$-1 in non-stressed cells (Fig. 3B) to that of $H1^S$-1 and $H1^S$-2, both ~40%, in the heat-shocked cells (Fig. 4A). The apparent increase in signal percentage from $H1^S$-1 after induction also was noted

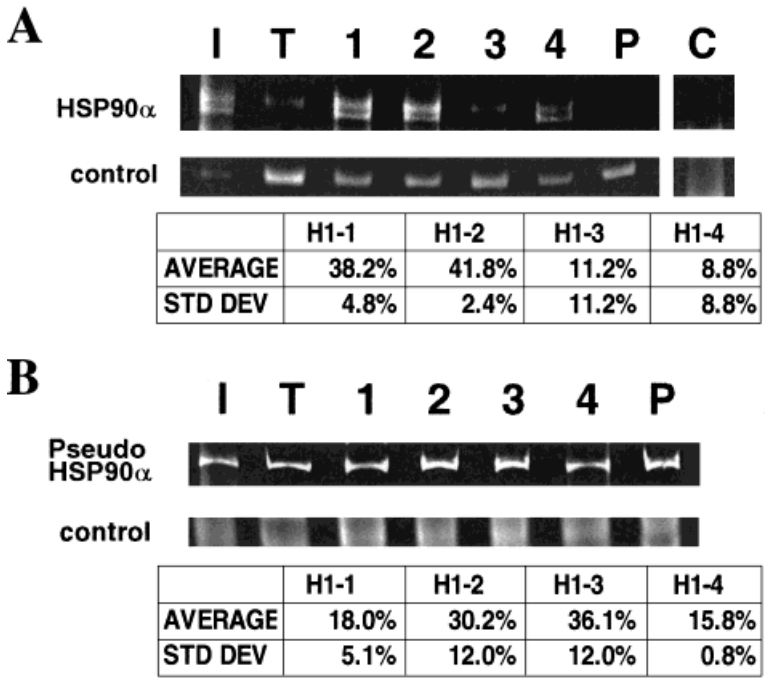

	H1-1	H1-2	H1-3	H1-4
AVERAGE	38.2%	41.8%	11.2%	8.8%
STD DEV	4.8%	2.4%	11.2%	8.8%

	H1-1	H1-2	H1-3	H1-4
AVERAGE	18.0%	30.2%	36.1%	15.8%
STD DEV	5.1%	12.0%	12.0%	0.8%

Fig. 4. PCR analysis upon Heat Shock Induction. Average SIPs and sample gels for the HSP90α (**A**) functional gene and (**B**) pseudogenes after incubation of the cells at 42°C for 1.5 to 2 h prior to formaldehyde crosslinking of the chromatin. PCR amplification procedures and legend abbreviations are identical to Figure 1. The doublet banding pattern seen in (A) was an artifact of the run.

in fetal fibroblasts [Parseghian et al., 2000] and was interpreted to represent additional selective removal of subtypes upon induction, specifically $H1^S$-3, leaving a residual amount of $H1^S$-1 on the gene to give rise to a basal level of chromatin condensation. A comparison of SIPs from adult material showed a significant decrease of $H1^S$-3 (from 46.2 to 11.2%) after heat-shock. However, unlike fetal cells, the apparent increase in signal from $H1^S$-1 is not as great due to the apparent increase in $H1^S$-2. The increased presence of $H1^S$-2, reminiscent of inactive chromatin, may correlate with a reduction in transcriptional induction in the adult fibroblast line. The results for inactive pseudogenes, where a more heterogenous subtype content continues to prevail after heat shock, are comparable for adult (Fig. 4B) and fetal cells [Parseghian et al., 2000].

It is noteworthy that a similar remodelling of subtypes has been observed for FGFR-3 upon heat shock (Fig. 5). As mentioned earlier, induction of this FGF receptor variant was noted after heat shock in both cell strains under study (Fig. 5A). Like HSP90α, there is a shift in the subtype content of FGFR-3 in non-stressed cells (Fig. 1B) to a predominance of $H1^S$-1 and $H1^S$-2 in the stressed adult cell line (Fig. 5B).

Transcriptional attenuation of heat shock genes with aging has been well-documented in several tissues including fibroblasts [Liu et al., 1989a], hepatocytes [Heydari et al., 1993], lymphocytes [Jurivich et al., 1997], lung [Fargnoli et al., 1990], and neural tissue [Brown and Gozes, 1998]. This phenomenon has been implicated in the declining ability of aging organisms to maintain homeostasis under conditions of environmental stress [for reviews, see Holbrook and Udelsman, 1994; Liu et al., 1996]. A diminished heat shock response is neither due to the proliferational state of the fibroblasts nor to an increased degradation of HSPs in older cells [Luce and Cristofalo, 1992].

As targets for a reduction in expression after heat shock, researchers have focused on the heat shock transcription factor-1 (HSF1) and its interaction with an HSP-specific promotor sequence, the heat shock element (HSE). A decline in HSF1 production with aging was ruled out in earlier studies demonstrating constant protein levels in adrenal gland tissue from young and old rats [Fawcett et al., 1994]. Several laboratories report that attenuation is due to an age-dependent reduction in HSF1 binding to the HSE [Choi et al., 1990; Heydari et al., 1993; Fawcett et al., 1994]. Neither structural alterations with age nor de novo synthesis of a defective HSF1 have been found [Choi et al., 1990]. However, it has been suggested that either modification-dependent activation is defective (such as phosphorylation) or there is the presence of an as yet uncharacterized

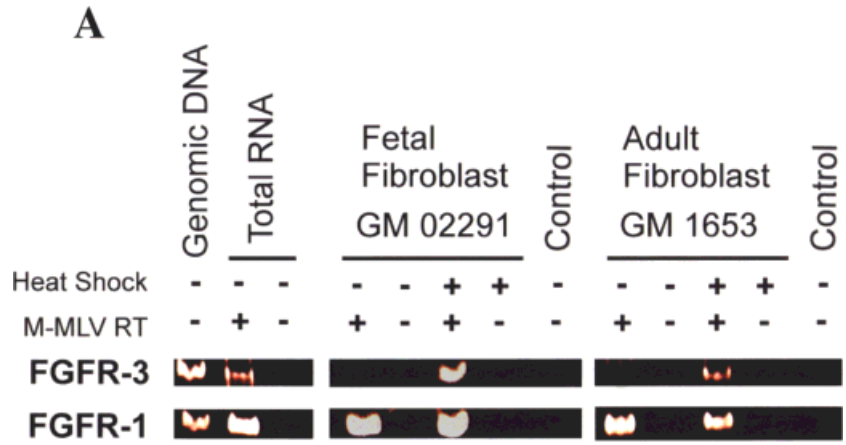

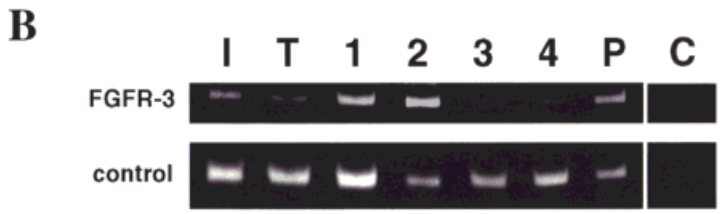

	H1-1	H1-2	H1-3	H1-4
AVERAGE	51.8%	48.2%	0.0%	0.0%
STD DEV	7.3%	7.3%	0.0%	0.0%

Fig. 5. Analysis of FGFR-3. **A:** Reverse-transcriptase PCR (RT-PCR) analysis of FGFR-3 induction in the two cell strains studied. RNA isolation and analysis are detailed in Parseghian et al. [2000]. Briefly, total RNA was extracted from both cell strains and transcribed by 100 U of Moloney murine leukemia virus reverse transcriptase (M-MLV RT). The resulting single-stranded DNA was then amplified by PCR and the product electrophoresed on a 6% acrylamide gel before visualization by ethidium bromide staining [Parseghian et al., 2000]. Controls include duplicate reactions with and without M-MLV RT, two positive controls using Genomic DNA and Total RNA from human fibroblasts, and a negative Control lacking DNA and RNA in the reaction mixture. **B:** Average SIPs and a sample gel for the FGFR-3 gene after heat shock of the adult fibroblast cells. A pixel-by-pixel analysis of the signal intensity from each band was conducted by digitizing the gels. Each of the resulting four subtype values (minus the preimmune's signal value) were totalled and the SIP for each determined. PCR amplification procedures and legend abbreviations are identical to Figure 1.

dominant inhibitor that interferes with HSF1 binding to the HSE [Choi et al., 1990].

Recently Jurivich et al. [1997] reported a disruption of HSF1 binding in HeLa cell extracts upon addition of the whole cell extracts from heat-shocked and non heat-shocked lymphocytes displaying an attenuated response. Jurivich et al. [1997] demonstrate that a putative inhibitor is generally present in tissue from older subjects (>75 years), is heat labile at 100°C, and is not a protease. The activity is lost upon stimulation of lymphocytes from quiescence to a proliferative state, then quickly restored within a few population doublings. It is not inconceivable that H1 is such an inhibitor. An extensive literature already exists describing the role of H1 in transcriptional repression [Shimamura et al., 1989; Croston et al., 1991; Laybourn and Kadonaga, 1991]. While the presence of an increased variety of H1 variants may generate a more condensed state of chromatin, specific subtypes may be responsible for maintaining transcriptional inactivity either individually or through interactions with other proteins. For instance, analysis of HSP90α at increasing cell passages lends support to this observation by finding a growing preponderance of $H1^S$-2 on the functional gene at a time when transcriptional induction begins to attenuate (Fig. 3B). Furthermore, heat shock induction of the very same gene in the adult fibroblast line results in the residual presence of $H1^S$-1 and $H1^S$-2, in marked contrast to induction of a fetal fibroblast line, where only

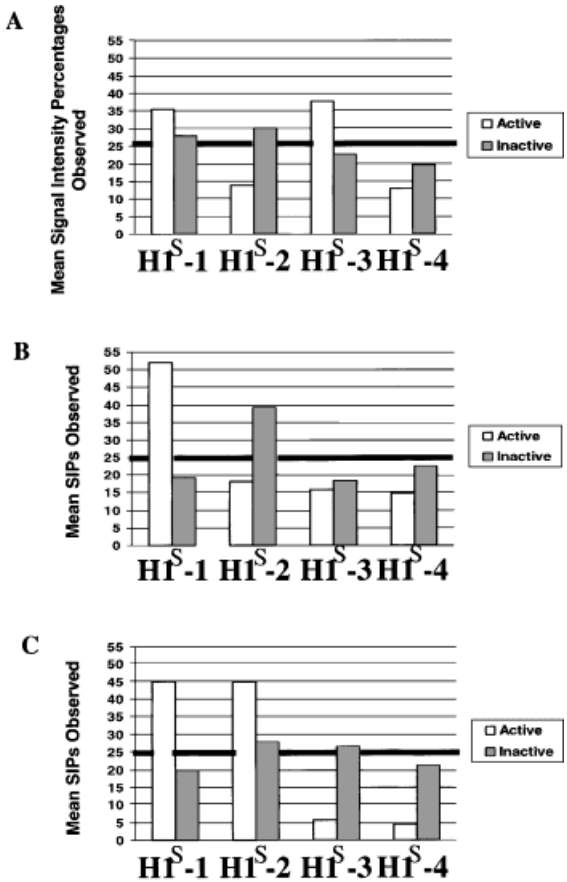

Fig. 6. Comparison of the mean signal intensity percentages observed for each subtype on active and inactive chromatin. The mean SIPs are also compared to the 25% mark expected with the null hypothesis and denoted by the dark line. **A:** Comparison of mean SIPs from the adult fibroblast line prior to heat shock. **B:** Comparison of mean SIPs from the fetal fibroblast line following heat shock. **C:** Comparison of mean SIPs from the adult fibroblast line following heat shock.

$H1^S$-1 is substantially detected (Fig. 6B). Hence, the lack of $H1^S$-2 dissociation from the DNA sequence in aging cells correlates with the reduction of heat shock induction.

ANOVA of SIPs

Confirmation of the subtype SIP distributions for each DNA sequence studied required repeated PCR or slot blot analysis. Although blocking agents were utilized during immunoprecipitation to minimize the general "stickiness" of chromatin, occasionally uncharacteristic SIP distributions occurred. Therefore, to determine the statistical significance of the differences observed in the SIP patterns of active and inactive chromatin, a comprehensive ANOVA was carried out by calculating the mean SIPs for each subtype and their deviations from the 25% benchmark of the null hypothesis (Fig. 6).

The null hypothesis is defined as a lack of significant SIP differences between active and inactive chromatin; thus, if the distribution of H1 subtypes throughout the nucleus is random, approximately equal signal intensities of about 25% should be observed from each of the four subtypes, regardless of the DNA sequence analyzed. In other words, the null hypothesis represents a state of maximum subtype heterogeneity where no single H1 variant predominates. An overall analysis of *differences* among SIP means for each of the four subtypes in active and inactive chromatin, in the absence of heat shock, produced a significant F score ($F = 2.63$, $P = 0.0140$), although this value was not as great as the F score for fetal fibroblasts ($F = 7.52$, $P = 0.0001$) [Parseghian et al., 2000]. The ANOVA F-test is a generalized t-test for the difference between two means allowing one to test the observed differences among the four SIP averages from the active chromatin with the four from the inactive. Graphically illustrating the mean SIPs demonstrates the diminished diversity of subtypes on actively transcribed sequences (Fig. 6A). ANOVA analysis of the inactive chromatin produces a pattern of four SIP means that fails to reject the null hypothesis ($F = 1.17$, $P = 0.3240$). However, this is not the case for analysis of the active chromatin, where the pattern of four SIP means leads to a strong rejection of the null hypothesis ($F = 7.65$, $P = 0.0004$).

This analysis was extended to chromatin following heat shock. To verify SIP shifts seen with HSP90α, the effects of heat shock induction on c-myc, FGFR-3, and IgKC were also evaluated using the adult and fetal fibroblast cells (data not shown). An overall analysis of *differences* among SIP means for each of the four subtypes in active and inactive chromatin following heat shock produced significant F scores in adult ($F = 6.03$, $P = 0.0010$), as well as fetal fibroblasts ($F = 4.57$, $P = 0.0065$). Graphical representations of the fetal (Fig. 6B) and adult (Fig. 6C) mean SIPs obtained with all of the genes after heat shock summarize the predominance of $H1^S$-1 on actively transcribed genes, the increased presence of $H1^S$-2 on those genes in adult fibroblasts, and the maintenance of a diverse subtype content on inactive DNA sequences.

TABLE I. Relative Presence of Total H1

Percentage intensity of input signal	Active chromatin (%)	Inactive chromatin (%)
Prior to heat shock...		
Adult fibroblasts	38.5	50.7
Fetal fibroblasts	11.4	35
Following heat shock...		
Adult fibroblasts	18.8	39.7
For telomeric sequences...	Telomeres	Inactive
Adult fibroblasts	13.8	50.7
Fetal fibroblasts	29	35

The relative presence of total H1 on various DNA sequences was determined by comparing the signal intensity values from anti-total H1 immunoprecipitates (minus the pre-immune signals). In order to account for the differences in signal from single and multi-copy sequences, the anti-total H1 values were normalized as a percentage of the intensity from each sequence's respective input signal.

Total H1 Content

The relative amounts of total H1 associated with each of the DNA sequences studied were estimated as previously described [Parseghian et al., 2000]. Briefly, signal generated with anti-total H1 for each of the sequences (minus the preimmune signal) is calculated as a percentage of the input DNA signal for the same sequence. Because the input DNA signal depends on the percentage a sequence is represented within the genome, the signal from the anti-total H1 precipitates can be normalized in this manner, allowing for comparisons between single and multi-copy sequences. This normalized value has been termed as the percentage intensity of input signal. This semi-quantitative analysis permits evaluation of the relative reduction in total H1 on actively transcribed sequences. In GM1653 fibroblasts, the *average* percentage intensity for actively transcribed genes was calculated from the set of c-myc data and was found to be 38.5% of the input signal whereas the *average* for inactive chromatin was 50.7%. These values are greater than the respective average percentages observed for active (11.4%) and inactive (35%) chromatin in a fetal fibroblast line (Table I), [Parseghian et al., 2000]. A reduced H1 content in active vs. inactive chromatin has been previously observed in *Tetrahymena* [Dedon et al., 1991] and chicken erythrocytes [Kamakaka and Thomas, 1990]. Upon exposure to heat shock, the average percentage intensities drop for active (18.8%) and inactive (39.7%) chromatin, indicating a reduction in total H1 content for all sequences. It is noteworthy that, despite this reduction, a heterogenous distribution of subtypes remained present on the inactive sequences (Fig. 4B). In addition, the average percentage of intensity of the input signals for both active and inactive chromatin, upon heat shock, is still greater in the adult cell line compared to the unstressed fetal cell line. Thus, the relative amount of H1 retained on the DNA of heat-shocked adult cells is greater than that found on unstressed fetal cells. Although the relative signal intensities are greater for inactive chromatin, they do not approach 100% due to the inefficiency inherent in immunoprecipitation.

In light of the unexpected SIP pattern observed on telomeres, the average percentage of intensity of input signal was determined solely for telomeric sequences and compared to the results for all inactive chromatin (Table I). The average percentage for telomeres in adult fibroblasts was 13.8%, far less than the overall average for inactive chromatin at 50.7%. A similar analysis of telomeric data from a fetal fibroblast line gave 29%, although not as large a difference, it was still less than the overall average for inactive sequences, 35% [Parseghian et al., 2000].

SUPPORTING OBSERVATIONS AND CONCLUSIONS

Figure 7 highlights our current model in light of the observations reported here. We have extended the earlier observations of others who have found a partial depletion of H1 on actively transcribed genes [Kamakaka and Thomas, 1990]. However, our published data and data presented here show that H1 depletion is subtype-specific and that there is a statistically significant difference in the subtype content of active and inactive DNA sequences (Table II). Although inactive chromatin contains all subtypes, the subtype content for actively

TABLE II. Relative Presence of H1 Subtypes on Various DNA Sequences

DNA sequence	Relative subtype distribution
Transcriptionally active	
PSD95	H1-1>H1-3>>H1-2 = H1-4
c-myc	H1-3>H1-1 = H1-4>>H1-2
HSP90α	H1-3>>H1-1>H1-2>>H1-4
HSP90α (after heat shock)	H1-1=H1-2>>>H1-3 = H1-4
Poised for Transcription	
FGFR-3	H1-3>H1-2 = H1-1>H1-4
Transcriptionally inactive	
LEF-1	H1-2>>H1-4>H1-3 = H1-1
IgKC	H1-2>>H1-4>H1-1>>H1-3
HSP90α pseudogenes	H1-2 = H1-3 = H1-4>H1-1
HSP90α pseudogenes (after heat shock)	H1-2 = H1-3>H1-4 = H1-1
Centromeric heterochromatin	
Centromeres	H1-1 = H1-2 = H1-3 = H1-4
Telomeric heterochromatin	
3.3 kb repeat (subtelomeric)	H1-3>>H1-2>H1-4>H1-1
Telomeres	H1-1>>>H1-2>H1-3 = H1-4

transcribed chromatin differs significantly from a random distribution.

Despite a more heterogenous presence of somatic subtypes on inactive vs. actively transcribed sequences, adult development appears to reduce these differences resulting in increased total H1 on active chromatin (Table I). However, this increase does not alter the general depletion of H1 on active vs. inactive sequences. In addition, adult active sequences exhibit greater subtype heterogeneity compared to their fetal counterparts, as evidenced

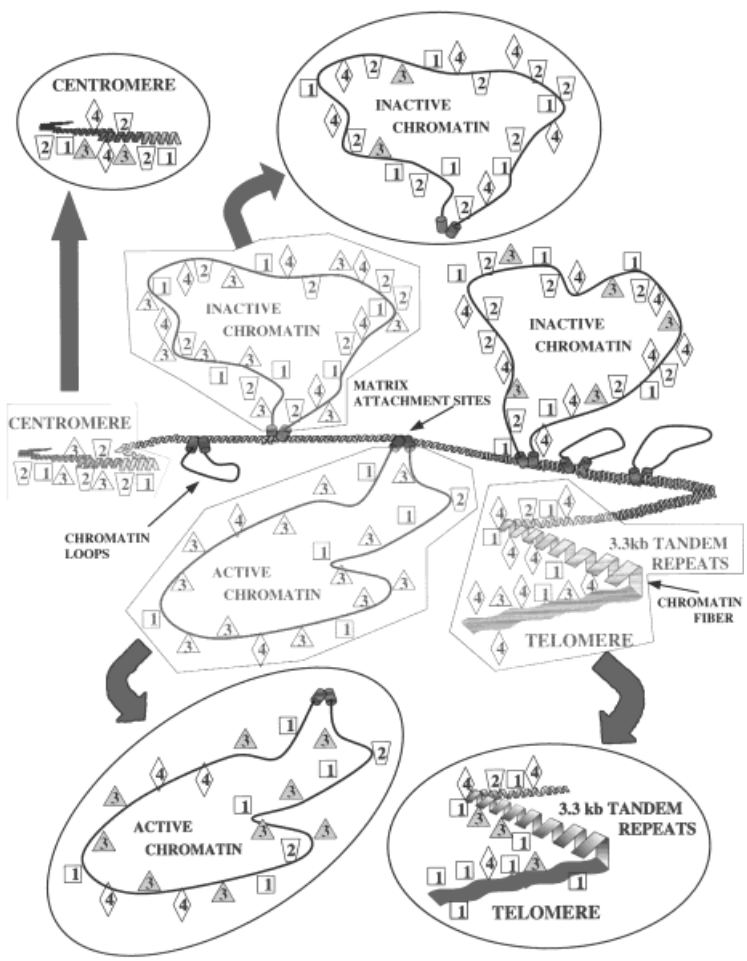

Fig. 7. Our current model of shifting somatic H1 subtype distributions in chromatin that accompany development and, possibly, aging. Faded regions illustrate subtype distribution on fetal chromatin, while the presence of H1 variants for the same regions in adult fibroblasts have been encircled. Triangles representing the distribution of subtype $H1^{s}$-3 have been shaded.

by the drop in statistical significance of the *differences* between the two transcriptional states in the fetal ($F = 7.52$, $P = 0.0001$) and adult ($F = 2.63$, $P = 0.0140$) fibroblasts. This increase in heterogeneity and total H1 throughout the nucleus, except at telomeres, may be reflected in vivo by increased condensation of chromatin [Chaurasia et al., 1996]. It may also be reflected in the irreversible arrest of cell proliferation, a characteristic of senescence [Campisi, 1996]. Indirect support for such a hypothesis was reported by Lu et al. [1997] who observed H1 modulation of DNA replication. Further analysis allowed them to characterize the process as one of H1 reducing the frequency of initiation by preventing the assembly of pre-replication complexes at replication origin sequences [Lu et al., 1998].

In a broader sense, such changes in the subtype content of active chromatin can be viewed as part of a continuum of changes in the H1 subtype content of nuclei during developmental transitions from blastula to neurula to differentiated somatic cells. These changes include a shift from the oocyte-specific H1, known as B4, which is considerably less basic and binds DNA less tightly than the somatic H1s [e.g. Dimitrov et al., 1993]. The shift to somatic H1s starts at the mid-blastula transition, is completed with the gastrula–neurula transition, and occurs concomitantly with decreases in DNA replication origins and increases in the length of S-phase [Callan, 1973]. This shift in subtype content has been correlated with increased transcriptional repression of those genes requiring RNA polymerase III [Dimitrov et al., 1993] and directly linked to a loss of mesodermal competence in *Xenopus* embryos [Steinbach et al., 1997]. One hypothesis is that, as an organism matures from embryonic to differentiated somatic cells, the inhibition of replication and repression of transcription are accompanied by an increasing condensation of chromatin due to accumulation of somatic H1s. A further shift in content occurring with the expression of differentiation-specific H1s, such as $H1^{o}$ and H5, only further the state of condensation in specific regions of chromatin [Roche et al., 1985; Brown et al., 1996]. In fact, several researchers have suggested that senescense resembles the process of terminal differentiation [Goldstein, 1990; Campisi, 1996] and others have shown that differentiation can continue to occur in fibroblast cells that have achieved mitotic arrest [Bayreuther et al., 1988].

Some of the observed shifts in somatic subtype content are supported by earlier observations with proliferating vs. quiescent cells [as reviewed in Parseghian and Hamkalo, 2001]. For example, Lennox and Cohen [1983] reported a decline in $H1^{S}$-3 expression in non-proliferating tissues of lung, liver, and kidney with increasing age and Piña et al. [1987] reported the gradual predominance of $H1^{S}$-4 in the nuclei of differentiating cerebral cortex neurons that have ceased to replicate. Meanwhile, $H1^{S}$-1 is reported to have the highest turnover rates, allowing it to replace other H1s independent of DNA synthesis [Pehrson and Cole, 1982] and probably accounting for its increased association with active chromatin from adult cells compared to fetal cells [compare Fig. 6A to 5A in Parseghian et al., 2000].

Such shifts in subtype content suggest the existence of a mechanism for remodeling the distribution of H1 variants. Indeed, recent studies of H1 mobility and exchange in the nucleus may shed light on such a mechanism. For instance, Misteli et al. [2000] have determined a residence time of approximately 220 sec for subtypes $H1^{S}$-1 and $H1^{o}$ on chromatin before their dissociation and diffusion to a new binding site. Their appears to be two "kinetic pools" of H1 within the nucleus, a mobile group and a more static group, with the latter more prevalent in heterochromatin [Misteli et al., 2000]. Possible facilitators of this mobility may be prothymosin α [Karetsou et al., 1998], NASP [Richardson et al., 2000], or the importin β/importin 7 heterodimer [Jäkel et al., 1999], each of which have been shown to bind and transport linker histones. Whatever the mechanism, H1 mobility is not driven by ATP-dependent chromatin remodelling complexes, however, phosphorylation may be a prerequisite, although the linker histones may not necessarily be the target of this modification [Lever et al., 2000].

To address complications of crosslinking due to H1 mobility, Jackson and Chalkley [1981] demonstrated that the immediate addition of formaldehyde to a mixture of chromatin and naked DNA prevented exchange of H1 from the chromatin to the DNA. We further analyzed the efficiency of our fixation process by crosslinking and sonicating cells followed by centrifugation of chromatin through 30 or 100 kDa Microcon

filtration tubes. Unfixed H1 (21 kDa) should elute through the 30 kDa filter; similarly, H1 monomers and multimeric aggregates should elute through the 100 kDa filter. However, Western analysis of the elutants did not detect H1 monomer or aggregates either by general protein stain or immunoblotting of the membrane (data not shown). Similar results were obtained with our analysis of heat-shocked cells. Therefore, it was concluded that the entire nuclear H1 content was crosslinked to chromatin via formaldehyde fixation. As for the possibility of H1 phosphorylation interferring with the crosslinking process, it is highly significant that $H1^S$-3 is present on active and inactive chromatin. Recently, Talasz et al. [1996] demonstrated that $H1^S$-3 is phosphorylated to a greater extent during each phase of the cell cycle than the other somatic subtypes. Yet, as the results show, we were able to effectively immunoprecipitate chromatin with the $H1^S$-3 specific antibody. Hence, the immunofractionation procedure employed with the fetal and adult fibroblast cell strains was neither compromised by phosphorylation nor H1 mobility.

Finally, shifts in subtype content could suggest the preferential association of some nuclear proteins with specific H1 subtypes. Hence, some subtypes may act as "platforms" that attract other nuclear proteins in much the same way the transcriptional machinery is assembled on a promoter. Recent evidence for such interactions has been presented by Liu et al. [1999] who describe the activation of DNA fragmentation factor-40 (DFF40) in response to apoptotic signals. DFF40 incurs DNA binding ability and an enhanced nuclease activity upon direct interaction with histone H1. This direct interaction was verified by immunoprecipitation of the complex using a monoclonal anti-H1. In order to test the "platform" hypothesis, it will be necessary to carry out Western blot analysis of immunofractionated chromatin to search for specific protein enrichments, and the Far Western analysis of subtypes with various nuclear proteins to determine the possibility of subtype-specific interactions.

ACKNOWLEDGMENTS

We wish to thank the following colleagues for supplying probes, PCR primers and expertise: Drs. Sara Winokur, Leslie Thompson, Dean Stathakis, Peter Bryant, Shoibal Datta, Hung Fan, Robert Moyzis, Judith Graff, Oliver Richards, Marian Waterman, Yolanda Bell and Ms. Karine Hovanes. We also thank members of the Hamkalo lab (Ms. Debra Harris, Dr. Nadja Dvorkin, Dr. Algis Jasinskas) and Drs. David Fouts and Jerry Manning for useful technical discussions.

REFERENCES

Ascenzi R, Gantt JS. 1999. Subnuclear distribution of the entire complement of linker histone variants in *Arabidopsis thaliana*. Chromosoma 108:345–355.

Bayreuther K, Rodemann HP, Hommel R, Dittmann K, Albiez M, Francz PI. 1988. Human skin fibroblasts in vitro differentiate along a terminal cell lineage. Proc Natl Acad Sci USA 85:5112–5116.

Bedoyan JK, Lejnine S, Makarov VL, Langmore JP. 1996. Condensation of rat telomere-specific nucleosomal arrays containing unusually short DNA repeats and histone H1. J Biol Chem 271:18485–18493.

Brown IR, Gozes I. 1998. Stress genes in the nervous system during development and aging diseases. In: Csermely P, editor. Stress of life: from molecules to man. New York: N.Y. Academy of Sciences. p 123–128.

Brown DT, Alexander BT, Sittman DB. 1996. Differential effect of H1 variant overexpression on cell cycle progression and gene expression. Nucleic Acids Res 24:486–493.

Burfeind P, Hoyer-Fender S, Doenecke D, Tsaousidou S, Engel W. 1992. Expression of a histone H1 gene (H1.1) in human testis and Hassall's corpuscles of the thymus. Thymus 19:245–251.

Callan HG. 1973. DNA replication in the chromosomes of eukaryotes. Cold Spring Harbor Symp Quant Biol 38: 195–203.

Campisi J. 1996. Replicative senescence: an old lives' tale? Cell 84:497–500.

Case JT, Wallace DC. 1981. Maternal inheritance of mitochondrial DNA polymorphisms in cultured human fibroblasts. Som Cell Genet 7:103–108.

Chadee DN, Taylor WR, Hurta RAR, Allis CD, Wright JA, Davie JR. 1995. Increased phosphorylation of histone H1 in mouse fibroblasts transformed with oncogenes or constitutively active mitogen-activated protein kinase kinase. J Biol Chem 270:20098–20105.

Chaurasia P, Mukherjee S, Thakur MK. 1996. Age-related analysis of EcoRI generated satellite DNA-containing chromatin of rat liver. Biochem Mol Biol Int 40:1261–1270.

Choi HS, Lin Z, Li B, Liu AYC. 1990. Age-dependent decrease in the heat-inducible DNA sequence-specific binding activity in human diploid fibroblasts. J Biol Chem 265:18005–18011.

Croston GE, Kerrigan LA, Lira LM, Marshak DR, Kadonaga JT. 1991. Sequence-specific antirepression of histone H1-mediated inhibition of basal RNA polymerase II transcription. Science 251:643–649.

d'Adda di Fagagna F, Hande MP, Tong WM, Lansdorp PM, Wang ZQ, Jackson SP. 1999. Functions of poly(ADP-ribose) polymerase in controlling telomere length and chromosomal stability. Nat Genet 23:76–80.

D'Erme M, Zardo G, Reale A, Caiafa P. 1996. Co-operative interactions of oligonucleosomal DNA with the H1e histone variant and its poly(ADP-ribosyl)ated isoform. Biochem J 316:475–480.

de Murcia G, Huletsky A, Lamarre D, Gaudreau A, Pouyet J, Daune M, Poirier GG. 1986. Modulation of chromatin superstructure induced by poly(ADP-ribose) synthesis and degradation. J Biol Chem 261:7011–7017.

Dedon PC, Soults JA, Allis CD, Gorovsky MA. 1991. Formaldehyde cross-linking and immunoprecipitation demon strate developmental changes in H1 association with transcriptionally active genes. Mol Cell Biol 11: 1729–1733.

Dimitrov S, Almouzni G, Dasso M, Wolffe AP. 1993. Chromatin transitions during early *Xenopus* embryogenesis: changes in histone H4 acetylation and in linker histone type. Dev Biol 160:214–227.

Fargnoli J, Kunisada T, Fornace AJ, Jr., Schneider EL, Holbrook NJ. 1990. Decreased expression of heat shock protein 70 mRNA and protein after heat treatment in cells of aged rats. Proc Natl Acad Sci USA 87:846–850.

Fawcett TW, Sylvester SL, Sarge KD, Morimoto RI, Holbrook NJ. 1994. Effects of neurohormonal stress and aging on the activation of mammalian heat shock factor 1. J Biol Chem 269:32272–32278.

Goldstein S. 1990. Replicative senescence: the human fibroblast comes of age. Science 249:1129–1133.

Hannon R, Bateman E, Allan J, Harborne N, Gould H. 1984. Control of RNA polymerase binding to chromatin by variations in linker histone composition. J Mol Biol 180:131–149.

Hayflick L, Moorhead PS. 1961. The serial cultivation of human diploid cell strains. Exp Cell Res 25:585–621.

Hebbes TR, Thorne AW, Crane-Robinson C. 1988. A direct link between core histone acetylation and transcriptionally active chromatin. EMBO J 7:1395–1402.

Heydari AR, Wu B, Takahashi R, Strong R, Richardson A. 1993. Expression of heat shock protein 70 is altered by age and diet at the level of transcription. Mol Cell Biol 13:2909–2918.

Hickey E, Brandon SE, Smale G, Lloyd D, Weber LA. 1989. Sequence and regulation of a gene encoding a human 89-kilodalton heat shock protein. Mol Cell Biol 9:2615–2626.

Holbrook NJ, Udelsman R. 1994. Heat shock protein gene expression in response to physiologic stress and aging. In: The biology of heat shock proteins and molecular chaperones. Cold Spring Harbor, NY: Cold Spring Harbor Laboratory Press. p 577–593.

Huletsky A, de Murcia G, Muller S, Hengartner M, Menard L, Lamarre D, Poirier GG. 1989. The effect of poly(ADP-ribosyl)ation on native and H1-depleted chromatin: a role of poly(ADP-ribosyl)ation on core nucleosome structure. J Biol Chem 264:8878–8886.

Innis MA, Gelfand DH. 1990. Optimization of PCRs. In: PCR protocols: a guide to methods and applications. New York: Academic Press. p 3–12.

Jackson V, Chalkley R. 1981. A new method for the isolation of replicative chromatin: selective deposition of histone on both new and old DNA. Cell 23:121–134.

Jurivich DA, Qiu L, Welk JF. 1997. Attenuated stress responses in young and old human lymphocytes. Mech Age Dev 94:233–249.

Jäkel S, Albig W, Kutay U, Bischoff FR, Schwamborn K, Doenecke D, Görlich D. 1999. The importin β/importin 7 heterodimer is a functional nuclear import receptor for histone H1. EMBO J 18:2411–2423.

Kamakaka RT, Thomas JO. 1990. Chromatin structure of transcriptionally competent and repressed genes. EMBO J 9:3997–4006.

Karetsou Z, Sandaltzopoulos R, Frangou-Lazaridis M, Lai C-Y, Tsolas O, Becker PB, Papamarcaki T. 1998. Prothymosin α modulates the interaction of histone H1 with chromatin. Nucleic Acids Res 26:3111–3118.

Laybourn PJ, Kadonaga JT. 1991. Role of nucleosomal cores and histone H1 in regulation of transcription by RNA polymerase II. Science 254:238–245.

Lennox RW, Cohen LH. 1983. The histone H1 complements of dividing and nondividing cells of the mouse. J Biol Chem 258:262–268.

Lever MA, Th'ng JPH, Sun X, Hendzel MJ. 2000. Rapid exchange of histone H1.1 on chromatin in living human cells. Nature 408:873–876.

Liu AYC, Lin Z, Choi HS, Sorhage F, Li B. 1989a. Attenuated induction of heat shock gene expression in aging diploid fibroblasts. J Biol Chem 264:12037–12045.

Liu AYC, Bae-Lee MS, Choi H-S, Li B. 1989b. Heat shock induction of HSP89 is regulated in cellular aging. Biochim Biophys Acta 162:1302–1310.

Liu AYC, Lee Y-K, Manalo D, Huang LE. 1996. Attenuated heat shock transcriptional response in aging: molecular mechanism and implication in the biology of aging. Exs 77:393–408.

Liu X, Zou H, Widlak P, Garrard WT, Wang X. 1999. Activation of the apoptotic endonuclease DFF40 (Caspase-activated DNAse or nuclease): oligomerization and direct interaction with histone H1. J Biol Chem 274:13836–13840.

Lu ZH, Sittman DB, Brown DT, Munshi R, Leno GH. 1997. Histone H1 modulates DNA replication through multiple pathways in *Xenopus* egg extract. J Cell Sci 110:2745–2758.

Lu ZH, Sittman DB, Romanowski P, Leno GH. 1998. Histone H1 reduces the frequency of initiation in *Xenopus* egg extract by limiting the assembly of pre-replication complexes on sperm chromatin. Mol Biol Cell 9:1163–1176.

Lu ZH, Xu H, Leno GH. 1999. DNA replication in quiescent cell nuclei: regulation by the nuclear envelope and chromatin structure. Mol Bio Cell 10:4091–4106.

Luce MC, Cristofalo VJ. 1992. Reduction in heat shock expression correlates with increased thermosensitivity in senescent human fibroblasts. Exp Cell Res 202:9–16.

Makarov VL, Lejnine S, Bedoyan JK, Langmore JP. 1993. Nucleosomal organization of telomere-specific chromatin in rat. Cell 73:775–787.

Misteli T, Gunjan A, Hock R, Bustin M, Brown DT. 2000. Dynamic binding of histone H1 to chromatin in living cells. Nature 408:877–881.

Moyzis RK, Buckingham JM, Cram LS, Dani M, Deaven LL, Jones MD, Meyne J, Ratliff RL, Wu J-R. 1988. A highly conserved repetitive DNA sequence, $(TTAGGG)_n$, present at the telomeres of human chromosomes. Proc Natl Acad Sci USA 85:6622–6626.

Norwood TH, Pendergrass WR, Sprague CA, Martin GM. 1974. Dominance of the senescent phenotype in heterokaryons between replicative and post-replicative human

fibroblast-like cells. Proc Natl Acad Sci USA 71:2231–2235.

Ozawa K, Murakami Y, Eki T, Soeda E, Yokoyama K. 1992. Mapping of the gene family for human heat-shock protein 90α to chromosomes 1, 4, 11, and 14. Genomics 12:214–220.

Parseghian MH, Hamkalo BA. 2001. A compendium of the histone H1 family of somatic subtypes: an elusive cast of characters and their characteristics. Biochem Cell Biol (in press).

Parseghian MH, Clark RF, Hauser LJ, Dvorkin N, Harris DA, Hamkalo BA. 1993. Fractionation of human H1 subtypes and characterization of a subtype-specific antibody exhibiting non-uniform nuclear staining. Chromosome Res 1:127–139.

Parseghian MH, Henschen AH, Krieglstein KG, Hamkalo BA. 1994a. A proposal for a coherent mammalian histone H1 nomenclature correlated with amino acid sequences. Protein Sci 3:575–587.

Parseghian MH, Harris DA, Rishwain DR, Hamkalo BA. 1994b. Characterization of a set of antibodies specific for three human histone H1 subtypes. Chromosoma 103:198–208.

Parseghian MH, Newcomb RL, Winokur ST, Hamkalo BA. 2000. The distribution of somatic H1 subtypes is nonrandom on active vs. inactive chromatin: distribution in human fetal fibroblasts. Chromosome Res 8:405–424.

Pehrson JR, Cole RD. 1982. Histone H1 subfractions and H1° turnover at different rates in nondividing cells. Biochemistry 21:456–460.

Pina B, Martinez P, Suau P. 1987. Changes in H1 complement in differentiating rat-brain cortical neurons. Eur J Biochem 164:71–76.

Richardson RT, Batova IN, Widgren EE, Zheng L-X, Whitfield M, Marzluff WF, O'Rand MG. 2000. Characterization of the histone H1-binding protein, NASP, as a cell cycle-regulated somatic protein. J Biol Chem 275:30378–30386.

Riquelme PT, Burzio LO, Koide SS. 1979. ADP ribosylation of rat liver lysine-rich histone in vitro. J Biol Chem 254:3018–3028.

Roche J, Gorka C, Goeltz P, Lawrence JJ. 1985. Association of histone H1° with a gene repressed during liver development. Nature 314:197–198.

Saccone S, DeSario A, Della Valle G, Bernardi G. 1992. The highest gene concentrations in the human genome are in telomeric bands of metaphase chromosomes. Proc Natl Acad Sci USA 89:4913–4917.

Shimamura A, Sapp M, Rodriguez-Campos A, Worcel A. 1989. Histone H1 represses transcription from minichromosomes assembled in vitro. Mol Cell Biol 9:5573–5584.

Smith S, Giriat I, Schmitt A, de Lange T. 1998. Tankyrase, a poly(ADP-ribose) polymerase at human telomeres. Science 282:1484–1487.

Steinbach OC, Wolffe AP, Rupp RAW. 1997. Somatic linker histones cause loss of mesodermal competence in *Xenopus*. Nature 389:395–399.

Talasz H, Helliger W, Puschendorf B, Lindner H. 1996. In vivo phosphorylation of histone H1 variants during the cell cycle. Biochemistry 35:1761–1767.

Thompson LM, Plummer S, Schalling M, Altherr MR, Gusella JF, Housman DE, Wasmuth JJ. 1991. A gene encoding a fibroblast growth factor receptor isolated from the Huntington disease gene region of human chromosome 4. Genomics 11:1133–1142.

Vamvakopoulos NC, Griffin CA, Hawkins AL, Lee C, Chrousos GP, Wang-Jabs E. 1993. Mapping the intron-containing human hsp 90α (HSPCAL4) gene to chromosome band 14q32. Cytogenet Cell Genet 64:224–226.

van Holde KE. 1988. Chromatin. In: Rich A, editor. New York: Springer-Verlag.

Wang Z-F, Sirotkin AM, Buchold GM, Skoultchi AI, Marzluff WF. 1997. The mouse histone H1 genes: gene organization and differential regulation. J Mol Biol 271:124–138.

Wiekowski M, Miranda M, Nothias J-Y, DePamphilis ML. 1997. Changes in histone synthesis and modification at the beginning of mouse development correlate with the establishment of chromatin mediated repression of transcription. J Cell Sci 110:1147–1158.

Winokur ST, Bengtsson U, Feddersen J, Mathews KD, Weiffenbach B, Bailey H, Markovich RP, Murray JC, Wasmuth JJ, Altherr MR, Schutte BC. 1994. The DNA rearrangement associated with facioscapulohumeral muscular dystrophy involves a heterochromatin-associated repetitive element: implications for a role of chromatin structure in the pathogenesis of the disease. Chromosome Res 2:225–234.

Yang TP, Hansen SK, Oishi KK, Ryder OA, Hamkalo BA. 1982. Characterization of a cloned repetitive DNA sequence concentrated on the human X chromosome. Proc Natl Acad Sci USA 79:6593–6597.